

## Ionization and Multifragmentation of $C_{60}$ by High-Energy, Highly Charged Xe Ions

T. LeBrun, H. G. Berry, S. Cheng,\* R. W. Dunford, H. Esbensen, D. S. Gemmell, and E. P. Kanter  
*Physics Division, Argonne National Laboratory, Argonne, Illinois 60439*

W. Bauer

*National Superconducting Cyclotron Laboratory, Michigan State University, East Lansing, Michigan 48824*  
 (Received 18 January 1994)

Ionization and multifragmentation have been observed in  $C_{60}$  molecules bombarded by  $Xe^{35+}$  and  $Xe^{18+}$  ions with energies in the range 420–625 MeV. The c.m. energies exceeded those used in previous studies by several orders of magnitude. We present the observed mass distribution of positively charged fragments together with a theoretical model indicating that the total interaction cross section contains roughly equal contributions from (a) excitation of the giant plasmon resonance, and (b) large-energy-transfer processes that lead to multiple fragmentation of the molecule

PACS numbers: 36.40.+d

The discovery [1] of the highly stable and symmetric quasispherical molecule  $C_{60}$  and related fullerenes has led to intense studies on a wide variety of the properties of this newly found form of carbon that can now be produced [2] in macroscopic quantities. Atomic collision techniques offer a powerful tool for investigating fullerene structures and dynamics and several such studies have already been reported [3]. In our experiments the center-of-mass energies exceed those used in previous work by several orders of magnitude. The high values of projectile velocity and charge state result in excitation and decay processes differing significantly from those seen in studies at lower energies (compare, for example, the recent work of Walch *et al.* [4]).

Our measurements were performed with  $^{136}Xe^{35+}$  or  $^{136}Xe^{18+}$  ions provided by Argonne's ATLAS accelerator at energies up to 625 MeV. These ions bombarded a  $C_{60}$  vapor target (density  $\sim 10^{10}/cm^3$ ) formed from 99.5% pure material heated to 475 °C in a two-stage stainless-steel oven. A time-of-flight (TOF) spectrometer system was located at 90° to the incident beam. Grids around the target region were biased with voltages to extract positively charged fragments and to inject them into a 20-cm-long gridded flight tube and thence into a microchannel plate detector. The total acceleration voltage was 6.9 kV. A "beam sweeper" allowed one 0.4-ns-wide beam pulse to reach the target every 10  $\mu s$ . TOF spectra were obtained using a "multihit" time digitizer with the "start" signal coming from the detector and the "stop" signal from the accelerator's timing system.

Figure 1 shows the TOF spectrum and its equivalent calibration in terms of  $M/Q$ , the ratio of fragment mass to charge. This spectrum is the sum of all eight channels in the time digitizer and thus reflects all positive fragments detected. Clusters ranging from single carbon atoms up to  $C_{60}^+$  are observed. The TOF spectrum also exhibits peaks attributable to light background gases ( $H_2O$ ,  $N_2$ ,  $O_2$ ,  $CO_2$ , etc.).

The peaks in Fig. 1 that correspond to interactions of the projectiles with  $C_{60}$  fall into three categories:

(1) Peaks due to singly, doubly, triply, and (possibly) quadruply ionized  $C_{60}$ . These "parent" peaks decrease in relative intensity towards higher charge states. Their narrowness reflects the small kinetic energy releases involved in the generation of these ions.

(2) Peaks corresponding to the successive losses of carbon pairs. Interestingly, these "pair-loss" peaks ( $C_{58}^{q+}$ ,  $C_{56}^{q+}$ ,  $C_{54}^{q+}$ , etc.) are stronger relative to their parent peaks for the higher charge states.

(3) Peaks corresponding to the sequence of singly charged fragments  $C_n^+$ , with  $n$  assuming all values from 1 to at least 19 (higher values then become indistinguishable from the multiply charged pair-loss peaks). These peaks alternate in intensity up to around  $n = 9$  with the odd-numbered peaks being more intense than the even-numbered. Above  $n = 9$ , the most intense peaks appear to be  $n = 11$ , 15, and probably 19. These intensity variations mirror those seen in other studies [5]. We refer to this series of peaks,  $C_n^+$ , as the "multifragmentation" peaks since we believe (see below) that they arise predominantly from events in which there is a catastrophic disintegration of the  $C_{60}$  molecule into many small fragments.

The manner in which energy is coupled into the  $C_{60}$  system from the passage of a highly charged fast ion (of velocity  $v$ ) can be expected to depend strongly on the impact parameter. The two principal distances of importance in discussing impact parameters are the mean radius  $\bar{R}$  (known [2] to be 3.55 Å) of the  $C_{60}$  "cage" on which are located the nuclei of the constituent carbon atoms, and the adiabatic distance [6]  $b_0 = \gamma \hbar v / E$  ( $= 10$  Å for  $E = 20$  eV), for the excitation of the giant dipole plasmon resonance of energy  $E$ . This collective excitation of the 240 valence electrons of the  $C_{60}$  molecule has been predicted [7] and measured [8] to have an energy of 20 eV and a FWHM of about 10 eV.

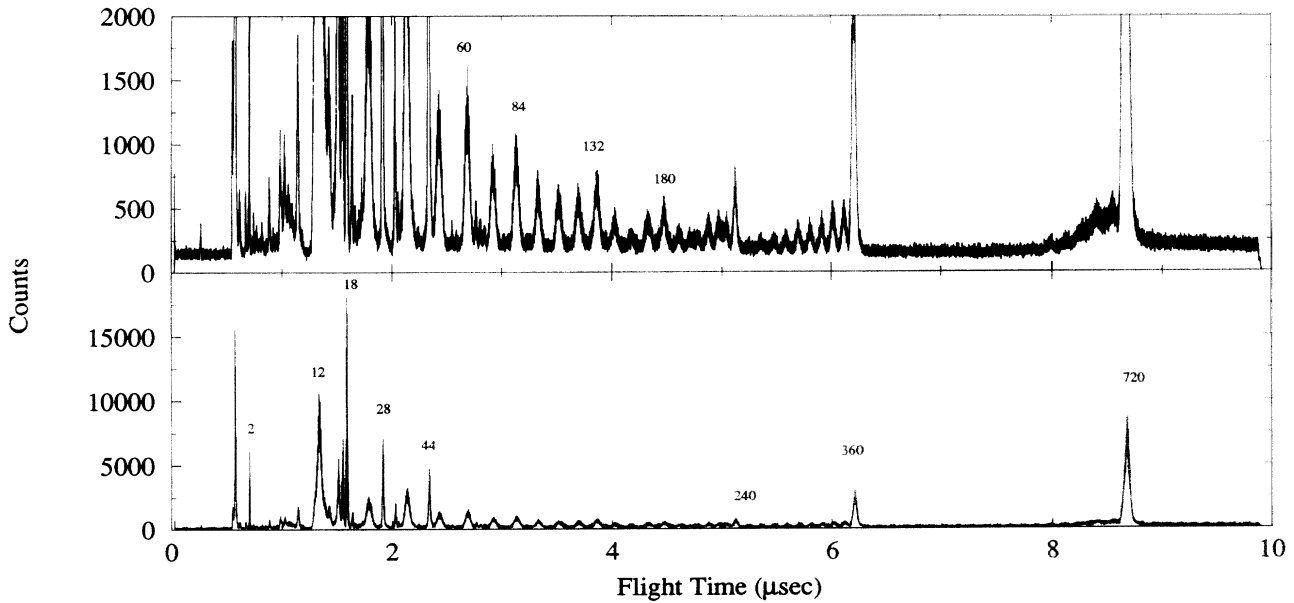


FIG. 1. Time-of-flight spectrum for positive fragments arising from bombardment of  $C_{60}$  by 625-MeV  $^{136}\text{Xe}^{35+}$  ions. The numbers given above some of the peaks are the ratios ( $M/Q$ ) of fragments mass (amu) to charge.

Preliminary to estimating the total interaction cross section, we consider the excitation of the giant dipole plasmon resonance by the Coulomb field of the xenon projectile. The effective number of plasmon excitations at an impact parameter  $b$  is

$$N(b) = \int dE \frac{f(E) 2Z_p^2 e^4}{E m v^2} \frac{1}{b^2} \times \left( \xi^2 K_1^2(\xi) + \frac{1}{\gamma^2} \xi^2 K_0^2(\xi) \right), \quad (1)$$

where  $\xi = Eb/\gamma\hbar v$ ,  $f(E)$  is the oscillator-strength distribution, and  $Z_p$  is the charge state of the xenon ion. This expression, obtained in first-order perturbation theory, is consistent with that for the average energy transfer to a harmonic oscillator [9]. The predicted [7, 10] oscillator strength is about 70. We have therefore parametrized the oscillator-strength distribution  $f(E)$  as a Gaussian, normalized to reproduce this and other known parameters of the resonance.

The excitation number  $N(b)$  is large for  $b \lesssim \bar{R}$ . The strength of the plasmon resonance, combined with the high charge state of the xenon ion, implies also that multiple excitations play an important role even at distances as big as the adiabatic distance  $b_0$ . To make a realistic estimate of cross sections, we describe the plasmon excitations in terms of a "coherent state" [11]. The multiplasmon excitation probabilities are then given by a Poisson distribution generated by  $N(b)$ . In particular, the probability for a one-plasmon excitation is  $N(b) \exp[-N(b)]$ , and the total excitation probability is  $1 - \exp[-N(b)]$ . These two probabilities are illustrated in Fig. 2(a).

The total excitation probability reaches unity at an impact parameter of about 7 Å, still far outside the radius

$\bar{R}$ . To determine the total interaction cross section, it is therefore not necessary to consider explicitly reactions at the smaller impact parameters where the xenon ion may interact with individual electrons, and we can simply write this cross section as

$$\sigma_{\text{exc}} = 2\pi \int_0^{\infty} db b \{1 - \exp[-N(b)]\}. \quad (2)$$

The single-plasmon excitation cross section is

$$\sigma_{\text{1pl}} = 2\pi \int_0^{\infty} db b N(b) \exp[-N(b)]. \quad (3)$$

This estimate is reasonable since all the cross section comes from impact parameters much larger than  $\bar{R}$  [cf. Fig. 2(a)]. The total interaction cross section obtained from the calculated values shown in Fig. 2(a) is 811 Å<sup>2</sup>, whereas the single-plasmon cross section is 387 Å<sup>2</sup>. i.e., 48% of the total.

Our model is valid for single-plasmon excitation involving large impact parameters where the linear-response and dipole approximations are valid. It can be expected to break down at smaller impact parameters where multiplasmon excitation occurs leading to multiple ionization, pair emission, and (at still smaller impact parameters) multifragmentation. The dominant decay mode of the single-plasmon excitation is thought to be via single electron emission [8, 12]. We therefore compare the calculated single-plasmon cross section [Eq. (3)] to our measured  $C_{60}^+$  yield. The dependence on beam energy is illustrated in Fig. 2(b) for the projectile charge state  $Z_p = 18$ . The weak dependence on beam energy is reproduced by the calculation. We were unable to determine accurate experimental cross sections. However, rough estimates based

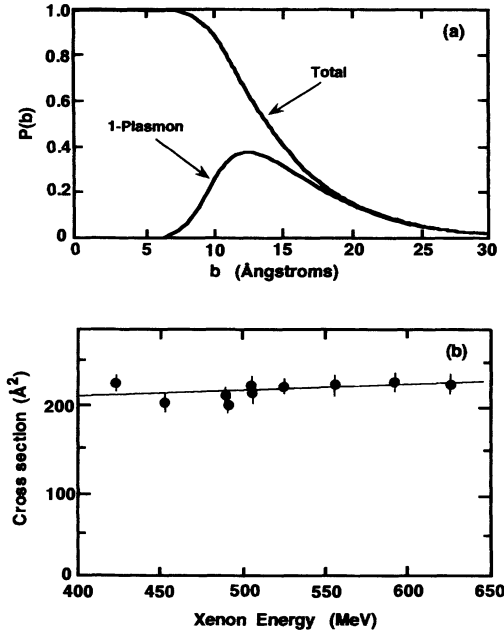


FIG. 2. (a) Calculated probabilities for the total interaction and for single-plasmon excitation as functions of the impact parameter,  $b$ , for 625-MeV  $^{136}\text{Xe}^{35+}$  ions. (b) Calculated [Eq. (3)] single-plasmon cross section (shown as a line) compared to the measured yield of  $C_{60}^+$  from  $C_{60}$  bombarded by  $^{136}\text{Xe}^{18+}$  ions in the energy range 420–625 MeV. The indicated errors are statistical only. The measured yields have been arbitrarily normalized to the calculation to display the similar energy variations. The measured and calculated yields agree within the overall experimental uncertainty [a factor of about 2 (see text)].

on the calculated vapor pressure, the integrated beam current, and taking into account the experimental geometry, detector efficiency, etc., agree with the calculated values within a factor of about 2. The slope of the calculated curve is insensitive to small variations in the total oscillator strength. We also considered the role of electron capture by the Xe ions as a production mechanism for  $C_{60}^+$  ions but at the high velocities (11–14 a.u.) of our beams, the charge-capture cross sections [13] are negligible compared to the cross sections for plasmon excitation.

At impact parameters less than about 7  $\text{\AA}$  where the energy deposition becomes large [see Eq. (1)], essentially all projectile-target interactions can be expected to result in multifragmentation. We have constructed a bond-percolation model to describe these fragmentation processes.  $C_{60}$  is represented as a collection of lattice sites located at the positions of the carbon atoms. Each site is connected to its three nearest neighbors via bonds. (In this calculation we do not distinguish between “single” and “double” bonds.) We assume that each xenon ion deposits excitation energy in proportion to its path length through the hollow fullerene structure. The energy is then rapidly distributed in a uniform manner over the whole  $C_{60}$  cluster. This leads to the breaking of individual bonds with

a probability proportional to the total energy deposition, which, in turn, is dependent on the impact parameter.

If we represent the fullerene as a spherical shell with mean radius  $\bar{R}$  and half-width  $\Delta R$ , then the impact-parameter dependence of the bond-breaking probability is given by

$$p(b) = \frac{p_0}{2\sqrt{\pi}w\Delta R} \times \int dr_{\perp} \left\{ \sqrt{[(\bar{R} + \Delta R)^2 - r_{\perp}^2]_+} - \sqrt{[(\bar{R} - \Delta R)^2 - r_{\perp}^2]_+} \right\} \times \exp[-(b - r_{\perp})^2/w^2], \quad (4)$$

where we introduce the symbol  $[a]_+ \equiv a$  ( $a \geq 0$ ),  $[a]_+ \equiv 0$  ( $a < 0$ ).  $w$  is the effective transverse width of the projectile, and  $p_0$  is the bond-breaking probability at  $b = 0$ .

After computing the breaking of the bonds by a given projectile, we employ a cluster recognition algorithm and identify the sites still connected via unbroken bonds as members of a cluster. We record the size of each cluster. This model is, except for considerations of the different reaction geometries involved, similar to a model of nuclear multifragmentation [14,15] used to explain production cross sections [16] for nuclear fragments emerging from heavy nuclei bombarded by protons with energies between 80 and 300 GeV.

Figure 3 shows the fragment-mass distribution calculated using this model and with parameters  $\Delta R = 0.35 \text{ \AA}$ ,  $w = 2 \text{ \AA}$ , and  $p_0 = 0.5$ . Our calculation reproduces the overall shape of the measured fragment mass spectrum. The calculation gives too little yield at high mass numbers because it does not take into account (a) the contributions from evaporative processes in which electrons and/or neutral carbon dimers are emitted following more gentle excitations (e.g., plasmon excitations), and (b) the known instability of odd-numbered heavy fragments which decay rapidly into even-numbered ones. The comparison shown in Fig. 3 assumes that the positive fragments are representative of all fragments emitted.

The symmetric shape of the measured mass distribution raises the question as to whether binary fragmentation plays a significant role. However, our coincidence measurements (not presented here) rule out this possibility.

Nuclear multifragmentation displays features similar to those observed in our data on fullerene disintegration, e.g., the phenomenon of limiting fragmentation (the fragmentation yield does not change much above a certain beam energy). Another common feature is the U-shaped fragment-mass spectrum.

Both experiment and calculation display a power-law falloff in the production cross sections for clusters of  $n$  carbon atoms,  $\sigma(C_n) \propto n^{-\lambda}$ , for  $n \leq 20$ . In experiment and calculation,  $\lambda \approx 1.3$ . This behavior is similar to the case of nuclear fragmentation [16], where one finds

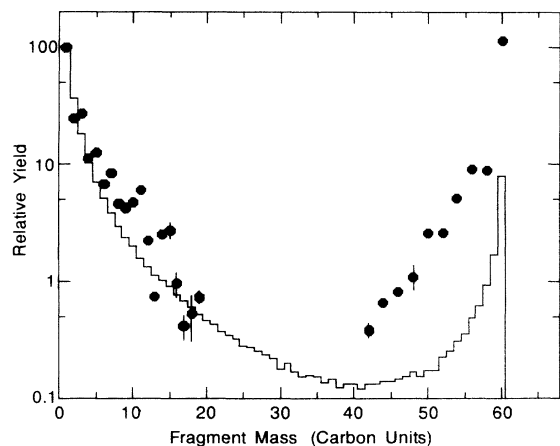


FIG. 3. Measured mass distribution (solid points) for positive fragments arising from  $C_{60}$  bombarded by 625 MeV  $^{136}\text{Xe}^{35+}$  ions. The histogram is the distribution calculated on the basis of a multifragmentation model (see text). The error bars are smaller than the points except where shown. The errors reflect statistical fitting errors and also any ambiguities in  $M/Q$  values (see Fig. 1). (The absence of experimental points for fragment masses between  $\sim 20$  and  $\sim 40$  is due to ambiguities of this sort.)

$\lambda \approx 2.6$  in inclusive (impact-parameter integrated) reactions. The power law is a consequence of the finiteness of the system and of the integration over different excitation energies in inclusive reactions [15]. The nuclear fragmentation data contain indications of a second-order phase transition in nuclear matter (albeit washed out due to finite-size effects), and at the critical point the apparent exponent  $\lambda$  has a minimum [14, 15]. Our  $\lambda$  value is significantly lower than the critical exponent ( $\tau = 2.0$ ) for two-dimensional infinite-size bond percolation and can be attributed to the finiteness and the periodic boundary conditions of our fullerene. Similar observations [17] have been recorded for nuclear systems. This opens an interesting avenue for further investigation of the disintegration of fullerenes, namely the possibility of observing the remnants of a phase transition in a finite-size two-dimensional object with periodic boundary conditions.

The present calculations do not reproduce the observed odd-even effect in the production cross sections for small  $n$ . This effect can be understood in terms of the binding energies of small carbon clusters. Calculations [18] show that  $C_2$  is bound by  $\approx 3.1$  eV/nucleon and  $C_3$  by  $\approx 5.5$  eV/nucleon, and that in general [5] the binding of small linear chains with  $2n$  members is weaker than those with  $2n \pm 1$ . The binding energy of a fragment  $E_b(n)$  enters into the final-state population via a factor  $\exp[-(E^* - E_b)/T]$ , where  $E^*$  is the mean excitation energy per carbon atom deposited in the fullerene, and  $T$  is the temperature of the fullerene at emission time. This explains qualitatively the odd-even effect in the observed cluster yields. Again, there is a parallel with nuclear fragmentation, for which the binding energies of the

fragments have similar effects on the observed fragment-mass distributions [19]. For cluster sizes above  $n \approx 10$ , we observe intensity oscillations with period 4, which we attribute to similar variations in the binding energies of carbon rings [5, 18].

This work was supported by the U.S. Department of Energy, Office of Basic Energy Sciences, under Contract No. W-31-109-ENG-38. One of us (W. B.) acknowledges support from an NSF Presidential Faculty Fellow Award. We gratefully acknowledge useful conversations with K. R. Lykke and the technical help of B. J. Zabransky and C. A. Kurtz.

\*Present address: Department of Physics and Astronomy, University of Toledo, Toledo, Ohio 43615

- [1] H. W. Kroto, J. R. Heath, S. C. O'Brien, R. F. Curl, and R. E. Smalley, *Nature* (London) **318**, 162 (1985).
- [2] W. Krätschmer, L. D. Lamb, K. Fostiropoulos, and D. R. Huffman, *Nature* (London) **347**, 354 (1990).
- [3] For reviews see, for example E. E. B. Campbell *et al.*, in *Nuclear Physics Concepts in Atomic Cluster Physics* (Springer, Berlin, 1992); and in Proceedings of the XVIII International Conference on the Physics of Electronic and Atomic Collisions, Aarhus, 21 July 1993 (to be published).
- [4] B. Walch, C. L. Cocke, R. Voelpel, and E. Salzborn, *Phys. Rev. Lett.* **72**, 1439 (1994).
- [5] See, for example, Von E. Dörnenburg and H. Hintenberger, *Z. Naturforsch.* **14A**, 765 (1959); G. von Helden, M.-T. Hsu, N. Gotts, and M. T. Bowers, *J. Phys. Chem.* **97**, 8182 (1993).
- [6] N. Bohr, *K. Dan. Vidensk. Selsk. Mat.-Fys. Medd.* **18**, No. 8 (1948).
- [7] G. F. Bertsch, A. Bulgac, D. Tomanek, and Y. Wang, *Phys. Rev. Lett.* **67**, 2690 (1991).
- [8] See, for example, I. V. Hertel, H. Steger, J. deVries, B. Weisser, C. Menzel, B. Kamke, and W. Kamke, *Phys. Rev. Lett.* **68**, 784 (1992); J. W. Keller and M. A. Coplan, *Chem. Phys. Lett.* **193**, 89 (1992).
- [9] J. D. Jackson, *Classical Electrodynamics* (Wiley, New York, 1962).
- [10] K. Yabana and G. F. Bertsch (private communication).
- [11] See, for example, E. Merzbacher, *Quantum Mechanics* (Wiley, New York, 1970), p. 367.
- [12] T. Drewello, W. Krätschmer, M. Fieber-Erdman, and A. Ding, *Int. J. Mass Spectrosc. Ion Proc.* **124**, R1 (1993).
- [13] A. S. Schlachter, J. W. Stearns, W. G. Graham, K. H. Berkner, R. V. Pyle, and J. A. Tanis, *Phys. Rev. A* **27**, 3372 (1983).
- [14] W. Bauer, D. R. Dean, U. Mosel, and U. Post, *Phys. Lett.* **150B**, 53 (1985); W. Bauer, U. Post, D. R. Dean, and U. Mosel, *Nucl. Phys.* **A452**, 699 (1986).
- [15] W. Bauer, *Phys. Rev. C* **38**, 1927 (1988).
- [16] A. Hirsch *et al.*, *Phys. Rev. C* **29**, 508 (1984).
- [17] L. Phair, W. Bauer, and C. K. Gelbke, *Phys. Lett. B* **314**, 271 (1993).
- [18] D. Tomanek and M. A. Schluter, *Phys. Rev. Lett.* **67**, 2331 (1991).
- [19] D. J. Fields, C. K. Gelbke, W. G. Lynch, and J. Pochodzalla, *Phys. Lett. B* **187**, 257 (1987).